Anal. Chem. 1995, 67, 4508–4513

In Situ Fourier Transform Infrared Spectroscopy of Molecular Adsorbates at Electrode–Electrolyte Interfaces: A Comparison between Internal and External Reflection Modes

I. T. Bae, M. Sandifer, Y. W. Lee, D. A. Tryk, C. N. Sukenik, and D. A. Scherson*

Ernest B. Yeager Center for Electrochemical Sciences and the Department of Chemistry, Case Western Reserve University, Cleveland, Ohio 44106

The vibrational properties of 2,5-dihydroxybenzyl mercaptan (DHBM) irreversibly adsorbed on gold electrodes have been examined in situ in aqueous 0.1 M $HClO_4$ by two different Fourier transform infrared (FT-IR) spectroscopic techniques: (i) potential difference attenuated total reflection FT-IR (PD-ATR-FT-IR), using a thin layer of gold (~4 nm) sputtered on a (thick layer) Au-patterned ZnSe internal reflection element as the electrode and (ii) PD-FT-IR (external) reflection absorption spectroscopy (PD-FT-IRRAS) on a solid Au electrode. The results obtained with both techniques, using the spectrum of the monolayer in the reduced state as a reference, were found to be nearly identical, displaying a set of negative- and positive-pointing features. The first set matched, within experimental error, the most prominent peaks observed in the ATR-FT-IR spectra of the DHBM monolayer using either pure water or 0.1 M $HClO_4$ as a reference. Furthermore, the positive-pointing features in the PD-FT-IR spectra, which correspond to the product of the electrochemical oxidation of irreversibly adsorbed DHBM, were consistent with the presence of a quinone-type moiety, as would be expected on the basis of chemical considerations. These observations indicate that, to the level of sensitivity of these two methodologies, the mode of adsorption and reactivity of DHBM (and probably a number of other species as well) is not appreciably affected by possible differences in the metal surface microstructure.

Since its inception over three decades ago, in situ infrared spectroscopy has provided extraordinary insights into a variety of interfacial processes, including the mechanisms of a number of electrochemical reactions,[1] modifications in the structure of irreversibly adsorbed species induced by changes in their oxidation state,[2] and, most notably, the effects of the applied potential and surface microstructure on the spectral properties of adsorbed carbon monoxide on metal electrodes.[3]

The vast majority of in situ infrared interfacial studies have been carried out in the external reflection absorption mode (IRRAS) using Fourier transform (FT) or, in most of the earlier studies, dispersive infrared instrumentation. Crucial to the success of this technique is the formation of a very thin layer of electrolyte between the infrared window and the electrode by pressing the flat surfaces of these two components against each other. This approach reduces the absorptivity due to the bulk electrolyte, which is particularly large in the case of aqueous solutions. Changes in the spectral properties of the interface induced by variations in the applied potential can then be obtained by taking the ratio of the single-beam spectra recorded at an arbitrary potential R from that acquired at a *reference* potential R_{ref}, without altering the electrode/window geometry (see below). This methodology has been shown to be exceptionally well-suited for studies involving irreversibly adsorbed carbon monoxide on Pt and other metal electrodes including single crystals, which can be electrochemically oxidized in aqueous electrolytes to yield *solution* phase carbon dioxide. Both these species display large, very sharp, nonoverlapping peaks in the IR region; hence, by an appropriate manipulation of the data, it is possible to obtain *absolute* spectra of the interface of remarkably good quality even for submonolayer coverages.

From a more general perspective, in situ IRRAS suffers from several disadvantages. In particular, mass transport in and out of the thin layer is controlled by migration in an electric field, rendering the electrolyte trapped therein *diffusionally decoupled* from the rest of the solution within the time scale required for the measurements. This effect can lead upon the passage of current to changes in the ionic composition,[4] including the *local* pH of weakly buffered solutions[5] and also to very slow rates of replenishment of uncharged reactants. In addition, the time constant of the cell is very long, due to the high resistivity of the thin electrolyte path; hence, the detection of short-lived transient species becomes essentially impossible. Lastly, a complete subtraction of bulk electrolyte contributions requires for these experiments to be carried out without disturbing the optics/cell arrangement, making it exceedingly difficult to obtain *absolute* spectra of a more general class of molecular adsorbates. Although

(1) (a) Bewick A.; Pons S. In *Advances in Infrared and Raman Spectroscopy*; Clark, R. J. H., Hester R. E., Eds.; Wiley-Heyden: London, 1985; Vol. 12. (b) Foley, J.; Korzeniewski, C.; Daschbach, J.; Pons, S. In *Electroanalytical Chemistry*; Marcel Dekker: New York, 1986; Vol. 14. (c) Ashley, K.; Pons, S. *Chem. Rev.* **1988**, *88*, 673.

(2) See, for example: (a) Sasaki, T.; Bae, I. T.; Scherson, D. A.; Bravo, B. G.; Soriaga, M. P. *Langmuir* **1990**, *6*, 1234. (b) Bae, I. T.; Huang, H.; Yeager, E. B.; Scherson, D. A. *Langmuir* **1991**, *7*, 1558.

(3) Chang, S.-C.; Weaver, M. J. *J. Phys. Chem.* **1991**, *95*, 5391, and references therein.

(4) Bae, I. T.; Xing, X.; Yeager, E. B.; Scherson, D. A. *Anal. Chem.* **1989**, *61*, 1164.

(5) Bae, I. T.; Scherson, D. A.; Yeager, E. B. *Anal. Chem.* **1990**, *62*, 45.

0003-2700/95/0367-4508$9.00/0 © 1995 American Chemical Society

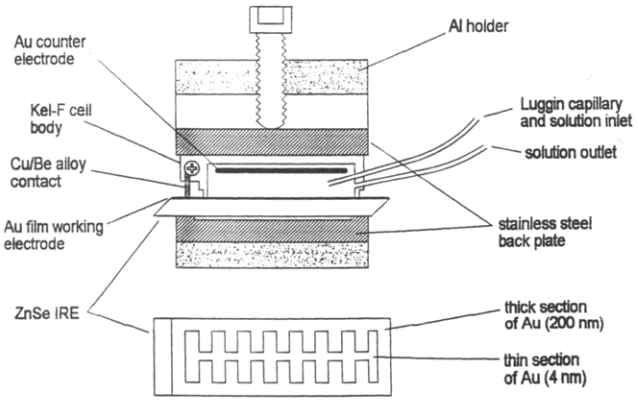

Figure 1. Schematic diagram of the spectroelectrochemical cell for in situ ATR-FT-IR measurements employed in these studies. Also shown in this figure is the top view of the patterned Au/ZnSe IRE electrode. The numbers in parentheses are the thicknesses of the Au deposits in the two sections.

efforts have been made to circumvent mass transport limitations by employing various forms of forced convection,[6] the hydrodynamic flow generated in such a constrained environment is ill-defined, and therefore, the conclusions emerging from such studies are mostly qualitative in nature. One of the strategies currently being explored in this laboratory involves the use of attenuated total reflection Fourier transform infrared (ATR-FT-IR) spectroscopy.[7] Although the virtues of this technique have been emphasized in various reviews,[8] only a few applications to in situ spectroelectrochemistry have been reported in the literature.[9,10] This specific technique shares the same surface selection rules applicable to metals in IRRAS, and hence, it can also provide information regarding molecular orientation.

This paper introduces in situ ATR-FT-IR as a probe of molecular adsorption on metal electrode surfaces in aqueous electrolytes, using 2,5-dihydroxybenzyl mercaptan (DHBM) adsorbed on Au as a model system. This species undergoes a reversible change in oxidation state in a potential region in which gold behaves as an ideal polarizable electrode and therefore appears to be especially suited for studies of this type. As will be shown, the potential difference (PD) ATR-FT-IR spectra of DHBM obtained for a patterned Au layer electrode sputtered on a ZnSe internal reflection element (IRE) was found to be nearly identical to the PD spectra of DHBM adsorbed on a solid Au electrode acquired in the more conventional FT-IRRAS configuration.

EXPERIMENTAL SECTION

In Situ Attenuated Total Reflection Fourier Transform Infrared Spectroscopy (ATR-FT-IR). Spectroelectrochemical Cell. A schematic diagram of a cell specifically designed for the acquisition of in situ ATR-FT-IR spectra is shown in Figure 1. The Au/ZnSe electrode was prepared by sputtering first a thick layer of Au (~200 nm) using a mask in the form of a *zipper* onto one of the large faces of a ZnSe IRE (50 × 20 × 3 mm, 45°, International Crystal). After removing the mask, a very thin layer of Au (4 nm) was sputtered onto the *whole* patterned surface of the prism (see Figure 1) to create, over certain areas, an electronically conducting surface connected to the thick Au overlayer. Such an approach makes it possible for a fraction of the evanescent wave to penetrate into the adjacent liquid media and thereby probe the vibrational properties of the Au electrode/electrolyte interface.[8]

The actual cell consists of a Kel-F piece in the form of an open rectangular cavity placed between the IRE and a stainless steel plate to yield a total cross-sectional area of the Au/ZnSe electrode exposed to the electrolyte of ~6 cm^2. Two Teflon tubes were press-fit to orifices drilled on the side of the Kel-F cell body. The lower orifice was used for injecting and removing solutions and to connect the main cell compartment to an external reference electrode compartment (not shown in the figure). After placing a second stainless steel plate in the back of the IRE, the whole cell assembly was mounted on a compressible aluminum bracket and attached to a custom-made optical plate for internal reflection measurements, which fits into the FT-IR spectrometer. The injection and removal of water and electrolyte into and from the cell during the adsorption, as well as all spectroelectrochemical measurements, were performed while the sample compartment of the spectrometer was purged with nitrogen *without disturbing the position of the cell assembly.*

Potential Difference (External) Fourier Transform Infrared Reflection Absorption Spectroscopy. Details regarding the PD-FT-IRRAS experiments, including a description of the CaF_2 dove-prism spectroelectrochemical cell, have been given in prior papers and will not be repeated here.[2]

Spectral Acquisition. FT-IR spectroscopic measurements were performed with a IBM IR-98 FT-IR spectrometer (Bruker 113v) equipped with a liquid nitrogen-cooled MCT detector at a 4-cm^{-1} resolution with unpolarized and p-polarized light for internal and external reflection, respectively. *In situ* spectra were acquired, either while sweeping the potential linearly after collecting a reference spectrum at a properly chosen potential or at fixed reference (ref) and fixed sampling (s) potentials (PD mode). Gains in signal-to-noise ratio were obtained by synchronizing the interferometric scan with a series of identical potential steps between two fixed values to collect *average* spectra at those potentials over short periods of time. In all cases, spectra are displayed in terms of $-\Delta R/R = (R_{ref} - R_s)/R_{ref}$, where R_s and R_{ref} are spectra recorded at the sampling and reference potentials, respectively. In the first method, spectral scans are coadded and then averaged, while the potential is scanned over a certain region; hence, R_s represents an *average* spectrum over both time *and* potential. Using this convention, and provided the interfacial process is reversible, positive-, and negative-pointing features can be associated with the interface at the sampling and reference potentials, respectively.

Adsorption of DHBM. Unless otherwise stated, the layer of DHBM was adsorbed on solid gold or sputtered Au surfaces by placing the electrode in contact with a 5 mM DHBM solution in water for ~5 min. Prior to the electrochemical and/or spectroelectrochemical experiments the electrode was rinsed thoroughly with water to remove nonadsorbed DHBM from the interface and then filled with 0.1 M $HClO_4$.

Electrochemistry. All electrochemical measurements were performed with instruments described elsewhere,[2] using a gold wire in the form of a coil as a counter and a reversible hydrogen electrode (RHE) as a reference.

(6) Roth, J. D.; Weaver, M. J. *Anal. Chem.* **1991**, *63*, 1603, and references therein.
(7) Ichino, T.; Cahan, B. D.; Scherson, D. *J. Electrochem. Soc.* **1991**, *138*, L59.
(8) Harrick, N. *Internal Reflection Spectroscopy*; Interscience Publishers: New York, 1967.
(9) Johnson, B. W.; Doblhofer, K. *Electrochim. Acta* **1993**, *38*, 695, and references therein.
(10) Parry, D. B.; Harris, J. M.; Ashley, K. *Langmuir* **1990**, *6*, 209

Synthetic Aspects. (a) General Procedures. NMR spectra were recorded in $CDCl_3$ using a Gemini 300 MHz NMR spectrometer and are reported in units of ppm. ^1H NMR and ^{13}C NMR spectra were referenced to $CHCl_3$ at 7.24 ppm and the center of the $CDCl_3$ triplet at 77.0 ppm, respectively. High-resolution mass spectra were acquired with a Kratos MS 25RFA spectrometer. FT-IR spectra for the synthetic work were recorded on a Perkin Elmer 16 PC. The HPLC equipment incorporated a Waters 590 pump, a Rheodyne 7125 injector, and a Waters 401 differential refractometer. TLC was performed on aluminum-backed 0.2-mm 60F254 plates from EM Science using phosphomolybdic acid for visualization. The pH was measured using a Fisher Accumet pH meter, Model 610. Column chromatography (flash) was done with silica gel (Aldrich, 230–400 mesh).

(b) Chemicals. Hexane and ethyl acetate (HPLC grade, Fisher) as well as ethyl alcohol (Aldrich), sodium hydroxide pellets (Aldrich), carbon tetrachloride (Fisher) *N*-bromosuccinimide (NBS; Aldrich), magnesium sulfate anhydrous (Aldrich), potassium thioacetate (Aldrich), methylene chloride (Aldrich), aluminum chloride (Aldrich), propanethiol (Aldrich), potassium thioacetate (Aldrich), sodium sulfate anhydrous (Fisher), reagent grade sodium chloride (Fisher), reagent grade ether (Fisher), and hexane (Fisher) used for column chromatography were all used as received. Benzoyl peroxide (Aldrich) was refrigerated and also used as received. Freshly opened bottles of DMF (Fisher) were employed. Concentrated hydrochloric acid (Fisher) was used as a reaction solvent and also to acidify reaction solutions.

Syntheses. (a) 2,5-Dimethoxymethylbenzene (1). In a dry three-neck 1-L round-bottom flask equipped with a magnetic stirring bar, two stoppers, a reflux condenser, and a N_2 inlet was placed 2,5-dihydroxymethylbenzene (49.6 g, 0.40 mol). To the flask was added 300 mL of ethanol, and the solution was slightly heated with a mantle until the solid dissolved. The heating mantle was then removed, and the solution was allowed to cool to room temperature. Over a period of 20 min, DMSO and 100 mL of an aqueous NaOH solution (~10 M) were added to the reaction mixture. The heat released was sufficient to bring the solution to boil. After this step was completed, sodium hydroxide (10 g, 0.25 mol) in 10 mL of water was added to the solution to make it alkaline. When the boiling subsided, the heating mantle was replaced and the reaction mixture refluxed for 7 h. The reaction mixture was checked by TLC and then transferred to a separatory funnel. The organic fraction was extracted with ether and washed with saturated aqueous NaCl solution. The resulting solution was dried with $MgSO_4$, filtered, and then concentrated on a Rotovap. The product was then subjected to flash chromatography (20% ether, 80% hexane), yielding a light yellow liquid: yield 53.3 g (93.9%); ^1H NMR δ 2.23 (s, 3H), 3.77 (s, 1H), 3.79 (s, 1H), 6.75 (m, 3H); ^{13}C NMR δ 16.33, 55.59, 55.82, 110.65, 110.84, 117.00, 127.76, 152.00, 153.32 ppm; IR (neat) 2927, 2807, 1601, 1516, 1471, 1048, 868, 788, 709 cm^{-1}.

(b) 2,5-Dimethoxybenzyl Bromide (2).[11] In a dry two-neck 250-mL round-bottom flask equipped with a reflux condenser, magnetic stirring bar, and a N_2 inlet was placed **1** (10.0 g, 0.066 mol). To the flask was added 180 mL of CCl_4, NBS (17.77 g, 0.099 mol), and a catalytic amount of benzoyl peroxide. The reaction mixture was refluxed for 2 h and checked by TLC. The succinimide was filtered off, and the resulting solution was concentrated on a Rotovap. The yellow liquid was crystallized from hexane. The product was obtained as a yellow solid and was used without any further purification: yield 15.2 g (99.2%); ^1H NMR δ 3.79 (s, 3H), 3.82 (s, 3H), 4.50 (s, 2H), 6.7–6.8 (m, 3H); ^{13}C NMR δ 28.9, 55.8, 56.3, 112.1, 115.1, 116.8, 130.9, 147.6, 154.0 ppm.

(c) 2,5-Dimethoxybenzyl Thioacetate (3). In a dry 500-mL round-bottom flask equipped with a stirring bar was placed **2** (9.38 g, 0.04 mol). To the flask was added potassium thioacetate (13.9 g, 0.12 mol) and 375 mL of DMF. The reaction solution was stirred for 2 h and checked by TLC. The mixture was diluted with water, poured into a separatory funnel, and extracted with ether. The ether extracts were combined and washed with a saturated aqueous NaCl solution. The resulting solution was dried with $MgSO_4$, filtered, and concentrated on a Rotovap. The crude product was purified by flash chromatography (30% ether, 70% hexane). The product was obtained as an amber liquid: yield 7.6 g (82.6%); ^1H NMR δ 2.30 (s, 3H), 3.73 (s, 3H), 3.77 (s, 3H), 4.08 (s, 2H), 6.74 (m, 2H), 6.89 (s, 1H); ^{13}C NMR δ 28.92, 30.19, 55.57, 55.90, 111.36, 113.11, 116.19, 126.74, 151.43, 153.25, 195.47 ppm; IR (neat) 2947, 2817, 2069, 1696, 1576, 1544, 1237, 1143, 963, 809, 719, 624 cm^{-1}.

(d) 2,5-Dihydroxybenzyl Thioacetate (4).[12] A dry, 250-mL round-bottom flask equipped with a magnetic stirring bar was charged with **3** (1.0 g, 4.4 mmol), $AlCl_3$ (2.4 g, 18 mmol), and 20 mL of CH_2Cl_2. The reaction mixture was stirred until the $AlCl_3$ was dissolved. The round-bottom flask was submerged in a ice bath, and 4 mL of propanethiol was added. The reaction mixture was warmed to room temperature and stirred for 2 h. The mixture was checked by TLC, and 25 mL of CH_3OH was carefully added. The resulting mixture was stirred for an additional 15 min and poured into a 500-mL flask with 200 mL of H_2O. After transferring the aqueous solution into a separatory funnel, the organic material was extracted with CH_2Cl_2, dried with Na_2SO_4, filtered, and concentrated on a Rotovap. The crude product was purified by HPLC (30% ethyl acetate, 70% hexane). The product obtained as an amber-colored viscous oil: yield 0.41 g (46.8%); ^1H NMR δ 2.35 (s, 3H), 3.99 (s, 2H), 5.47 (s, ^1H), 6.62–6.76 (m, 3H), 6.96 (s, 1H); ^{13}C NMR δ 28.94, 30.17, 116.23, 116.91, 118.25, 124.94, 147.74, 149.36, 200.26 ppm; IR (neat) 3386, 1676, 1511, 1457, 1207 cm^{-1}.

(e) 2,5-Dihydroxybenzyl Mercaptan (5). In a 100-mL round-bottom flask equipped with a magnetic stirring bar was dissolved **4** (0.71 g, 3.6 mmol) in concentrated HCl. The reaction was stirred for 5 h. The pH of the reaction mixture was adjusted to 3.90 with saturated aqueous sodium bicarbonate. The resulting mixture was poured in a separatory funnel. The product was extracted with CH_2Cl_2 and washed with a saturated aqueous NaCl solution. The combined CH_2Cl_2 extracts were dried over Na_2SO_4, filtered, and concentrated on a Rotovap. The crude product was purified by chromatography (80% ether, 20% hexane): yield 450 mg (80.9%); MS *m/e* 156.0245 (calcd), 156.0219 (found); melting range 125–127 °C; ^1H NMR δ 1.84 (t, 1H, J = 7.3 Hz), 3.69 (d, 2H, J = 7.3 Hz), 4.36 (s, 1H), 5.24 (s, 1H), 6.60–6.74 (m, 3H) ppm; ^{13}C NMR δ 46.33, 138.59, 139.67, 140.52, 153.02, 172.43 ppm; IR (KBr) 3263, 2603, 1465, 1380, 1248, 1205, 1160, 1096, 991, 881, 815, 770 cm^{-1}.

(11) Procedure modeled after that of: Tashiro, M.; Yamato, T. *J. Org. Chem.* **1985**, *50*, 2939.

(12) Procedure modeled after that of: Node, M.; Nishide, K.; Fuji, K.; Fujita, J. *J. Org. Chem.* **1980**, *45*, 4275.

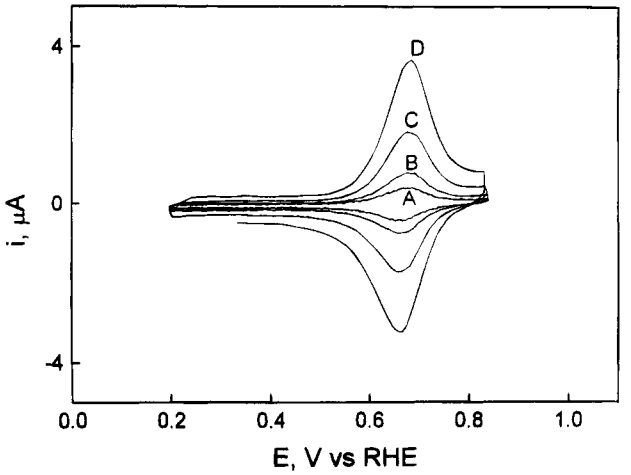

Figure 2. Cyclic voltammetry curves of irreversibly adsorbed DHBM on a solid gold electrode in neat 0.1 M $HClO_4$ recorded at 10 (A), 20 (B), 50 (C) and 100 mV/s (D) in a conventional electrochemical cell. Electrode area, 0.2 cm^2 (see text for details).

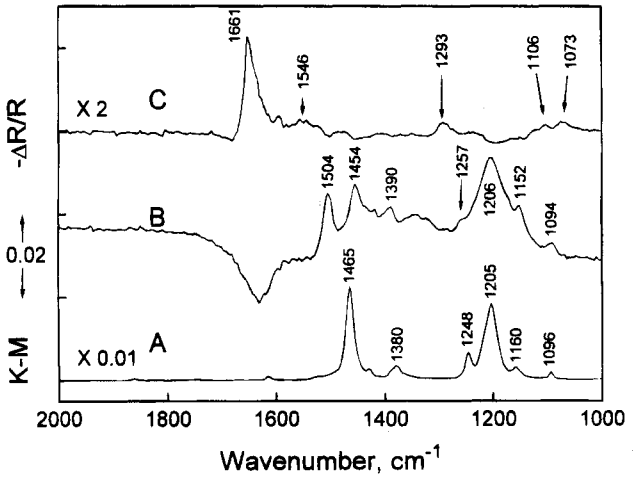

Figure 3. (A) Fourier transform infrared spectra of solid DHBM dispersed in ground KBr obtained in the diffuse reflectance mode. (B) *Absolute* ATR-FT-IR spectra of an irreversibly adsorbed layer of DHBM on a patterned Au/ZnSe electrode in water using the spectrum for the interface prior to DHBM adsorption in *water* as the reference. (C) In situ potential difference ATR-FT-IR spectra of the DHBM layer in curve B in 0.1 M $HClO_4$ obtained by the synchronization technique (see text) using a potential step between 0.4 and 0.85 V vs SCE and the *average* spectrum acquired at 0.4 V as the reference.

RESULTS AND DISCUSSION

The cyclic voltammetry of DHBM adsorbed on a solid gold electrode in neat 0.1 M $HClO_4$ yielded oxidation and reduction peaks at ~0.65 vs RHE (see Figure 2) separated by ~5 mV. These features are shifted by ~70 mV in the positive direction with respect to those reported for the closely related 2,5-dihydroxythiophenol (DHT) adsorbed on Au in the same electrolyte.[2] This is not surprising, since the direct attachment of sulfur to the ring in DHT stabilizes the resulting radical and thus lowers the potential required for the oxidation. As expected for an ideally behaved irreversibly adsorbed redox active species, a plot of the current at the peak (i_p) was found to be proportional to the scan rate (ν) in the range examined.

Prior to conducting spectroelectrochemical experiments, a spectrum of the Au/ZnSe interface was recorded in ultrapure water (R_{water}), which served as a reference for obtaining the *absolute* spectra of adsorbed DHBM at the Au/ZnSe water interface. The water in the cell was then replaced by a 5 mM DHBM aqueous solution, and a series of spectra were subsequently recorded as a function of time. The DHBM solution was then removed and the cell rinsed repeatedly with water to ensure that the resulting spectrum was indeed associated with the adsorbed and not (minor contributions due) to the solution phase form of the species. The spectra for the DHBM monolayer obtained *in water* after this procedure was completed (using R_{water} as the reference), which may be regarded as the *absolute* interfacial spectra of the DHBM layer (*in water*), is shown in curve B, Figure 3. As has been postulated in the literature, thiol-functionalized species, such as DHBM, bind via the sulfur to metal surfaces, such as, Au, Pt, Cu, and Ag; the lack of a S–H stretch at 2603 cm^{-1} in the spectrum is consistent with this view.

The *absolute* interfacial spectrum of adsorbed DHBM on Au/ZnSe in water bears close resemblance to that of the solid material dispersed in ground KBr by diffuse reflectance FT-IR (see curve A, Figure 3), except for the *splitting* of the 1465-cm^{-1} band in the solid into a doublet at 1504 and 1454 cm^{-1}. This phenomenon has also been observed in solution phase and therefore cannot be ascribed to a surface-type interaction. The water in the cell was then replaced by 0.1 M $HClO_4$ and a new *reference* spectrum, denoted simply as R, was recorded. Except for a large positive-pointing peak at ~1100 cm^{-1} due to perchlorate, the spectra

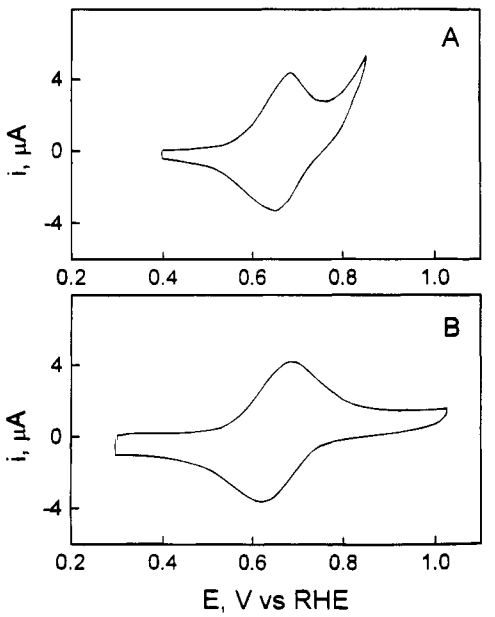

Figure 4. Cyclic voltammetry for the DHBM layer irreversibly adsorbed on the Au/ZnSe electrode which yielded the *absolute* spectrum shown in curve B, Figure 3, in 0.1 M $HClO_4$ (A) and for a similar DHBM layer adsorbed on a solid Au electrode in the spectroelectrochemical cell for external reflection FT-IR in the same electrolyte (B). Scan rate, 1 mV/s.

obtained for DHBM/Au/ZnSe in the electrolyte, using R_{water} as the reference (not shown in the figure), was the same as that observed for the DHBM monolayer in pure water.

The cyclic voltammetry for the DHBM monolayer irreversibly adsorbed on the Au/ZnSe electrode, given in panel A, Figure 4, was similar to that shown in Figure 2 and also to that recorded for DHBM on solid Au in the external reflection FT-IR cell (see panel B, Figure 4). The slight differences in peak separation in the latter case may be due to distortions induced by the cell geometry. The current observed at potentials more positive than ~0.75 V for the DHBM/Au/ZnSe interface, which overlaps with

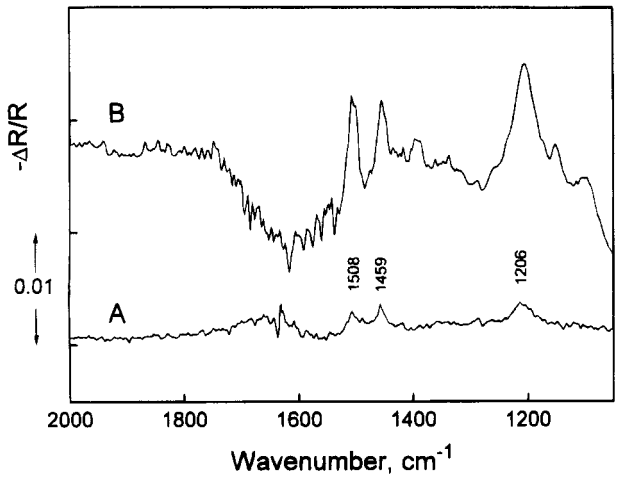

Figure 5. *Absolute* ATR-FT-IR spectra of an irreversibly adsorbed layer of DHBM on the bare ZnSe IRE in water using the spectrum for the interface prior to DHBM adsorption in *water* as the reference (curve A). Curve B shows the *absolute* spectrum of DHBM on Au/ZnSe in (B), Figure 3, for comparison.

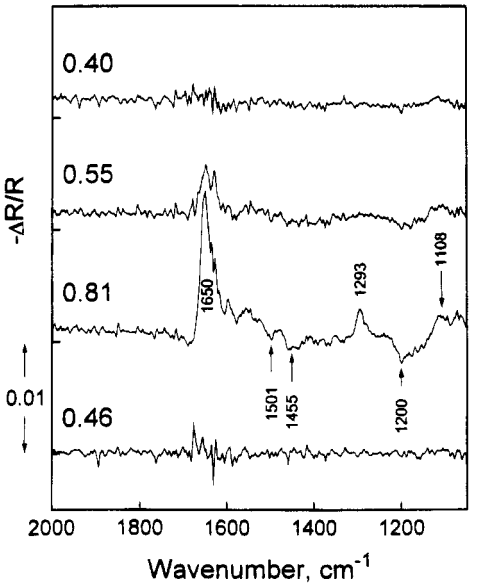

Figure 6. Series of potential difference spectra using the spectrum of the DHBM layer in curve B, Figure 3, in 0.1 M $HClO_4$ as a reference (denoted as R in the text) at 0.40 V (see above) obtained during a single voltammetric scan at 1 mV/s. The labels in each of the curves correspond to the average potential values during each spectral coaddition.

the tail end of the oxidation wave, is believed to be associated with the onset of the electrochemically induced dissolution of the underlying ZnSe. Integration of the area under the voltammetric peak, assuming a two-electron-transfer process, yielded a value equivalent to $\sim 2.5 \times 10^{-10}$ mol/cm^2 and, thus, more than 4 times smaller than that found for DHBM adsorbed on solid gold, 1.1×10^{-9} mol/cm^2. This value includes DHBM adsorbed on the thick Au area not probed by the evanescent IR beam and Au sections in the thin area in electrical contact with the rest of the electrode.[13]

The integrated voltammetric peak in Figure 4A, however, does not account for DHBM molecules adsorbed on thin Au-sputtered sections electrically isolated from the thick Au-patterned area of the IRE or on bare ZnSe. The affinity of DHBM for ZnSe was examined by comparing the spectrum of bare ZnSe *in water* before and after exposing the surface to the 5 mM DHBM solution by employing the same methodology described above. As shown in curve A, Figure 5, the *absolute* spectra of DHBM on bare ZnSe yielded peaks at 1508, 1459, and 1206 cm^{-1}, in agreement with the features observed for the *absolute* spectra of DHBM on Au/ZnSe (see curve B in this figure). As evidenced by the size of the signal, however, the amount of DHBM adsorbed on ZnSe is relatively small and cannot account for the large fraction of electrochemically inactive material detected by the IR beam. This indicates that a large fraction of DHBM is adsorbed on gold islands isolated electronically from the rest of the electrode.

An estimate of the relative amount of electrochemically vs nonelectrochemically active material *in the IR beam* could be obtained by acquiring ATR-FT-IR spectra as a function of potential during a linear scan as described below.

Figure 6 shows a series of PD ATR-FT-IR spectra acquired during a scan at 1 mV/s, using R at 0.40 V as a reference. The labels in each of the curves correspond to the average potential values during each spectral coaddition. As clearly indicated, prominent positive-pointing bands could be observed in a potential range in which the DHBM is expected to be fully oxidized. No spectral features could be discerned in the PD spectra of the interface after a complete voltammetric cycle (see curves for $V =$ 0.46 Vand $V = 0.40$ V), providing strong evidence that the redox process is fully reversible. These PD spectra also contain a series of negative-pointing bands at the same energies as those found in the *absolute* spectra of adsorbed DHBM, which are better resolved in the synchronized PD difference spectra in curve C, Figure 3.

These in situ ATR-FT-IR results are very similar to those observed in in situ FT-IRRAS measurements involving DHBM adsorbed on a solid Au electrode in 0.1 M $HClO_4$ using the same potential scan technique, as illustrated in Figure 7. An important difference, however, is the presence of a positive-pointing band at $\sim$1112 cm^{-1} (see Figure 7), which is associated with the migration of perchlorate into the thin layer (during the oxidation) to maintain electroneutrality. As clearly shown in the upper curve in Figure 7, ion migration is reversible as evidenced by the disappearance of the ClO_4^- peak upon fully reducing the adsorbate layer. Such electrolyte-related bands can overlap in certain cases with spectral features associated with products of electrochemical reactions and thereby restrict the usefulness of external FT-IRRAS for this type of application. An assignment of the most prominent bands observed in the in situ and powder spectra of DHBM can be found in ref 2a. In analogy with the behavior observed for DHT, and in line with chemical considerations, all spectral features are consistent with the oxidation of the surface-confined hydroquinone to yield the corresponding quinone. As mentioned above, a comparison of the size of the features in the *absolute* and PD ATR-FT-IR (see curves B and C in Figure 3) provides a measure of the amount of electrochemically active DHBM in the path of the beam. Based on these curves, it appears that sputtered Au electrodes of the type used in this study yield only 25–30% of all species adsorbed in electrical contact with the external circuit.

An increase in the size of the optically accessible electrochemically active area without losses in the total throughput can, in

(13) Also to be considered are contributions to the current due to molecules adsorbed on isolated Au deposits (or on bare ZnSe; see below) capable of undergoing changes in oxidation state by intermolecular electron transfer with species in contact with electrically connected areas of the Au overlayer. However, the experiments described in this work are not optimized to check for this possibility.

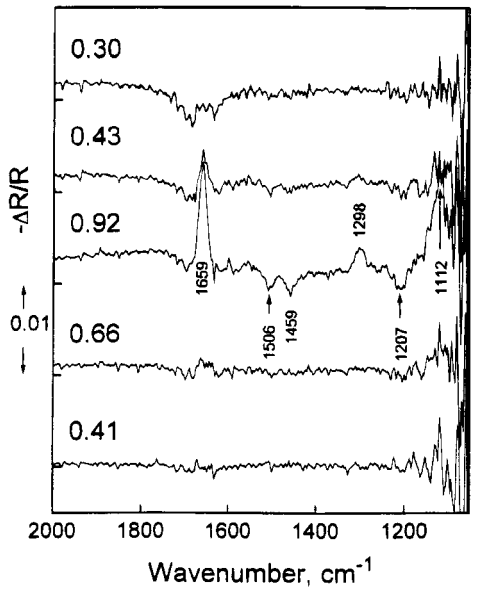

Figure 7. Series of in situ (external) potential difference FT-IRRAS spectra for DHBM irreversibly adsorbed on a solid Au electrode in 0.1 M $HClO_4$ using the same potential scan technique described in the caption of Figure 6.

principle, be achieved by creating an array of alternating thick and thin Au-coated segments of very small width, e.g., a few tenths of a millimeter. Various designs are currently being considered to explore the correlation between the spectroscopic and electrochemical responses.

From a quantitative viewpoint, two factors complicate a full analysis of in situ internal reflection data obtained with the experimental ATR arrangement employed in this work. First, the center of gravity of the bands is affected by the thickness of the metal layer. A clear illustration of this effect was given recently by Ishida and Griffiths,[14] who predicted theoretical shifts in the center of gravity of the water band at ~1640 cm^{-1} of ~10 cm^{-1} for bare Ge compared to Ge covered by a layer of Cu 15 nm in thickness in contact with bulk water. Second, thin layers of the type used in the present work are not of a uniform thickness but consist instead of interconnected islands. This type of metal structure can be responsible for enhancements in the band intensities, a phenomenon dubbed *surface-enhanced infrared absorption*.[15] Despite these uncertainties, in situ ATR-FT-IR can provide reliable information regarding various aspects of the structure of irreversible adsorbed layers that can help identify reaction pathways of electrochemical reactions and other interfacial processes as well.

(14) Ishida, K. P.; Griffiths, P. R. *Anal. Chem.* **1994**, *66*, 522.
(15) (a) Suzuki, Y.; Osawa, M.; Hatta, A.; Suetaka, W. *Appl. Surf. Sci.* **1988**, *33*, 875. (b) Osawa, M.; Ataka, K. *Surf. Sci. Lett.* **1992**, *262*, L118.

CONCLUDING REMARKS

The results presented in this study have opened new prospects for the use of internal reflection FT-IR as a sensitive in situ probe of adsorbed molecules on thin layers of gold and possibly other metals in aqueous electrolytes capable of yielding *absolute* interfacial spectra. As shown in this work, and despite the lack of an ideally designed patterned electrode, the spectral properties of a model redox-active irreversibly adsorbed species, DHBM, do not seem to be appreciably affected by differences in the nature of gold in the sputtered film compared to a massive specimen. The window of electrochemical stability of the rather ill-defined gold/ZnSe interface, at least in the fairly acidic environment involved in this work, seems to be limited to ~0.85 V vs RHE. Nevertheless, the possibility of designing cells with optimum current distribution, fast time response, and well-defined hydrodynamic flow will make it possible, in principle, to increase the sensitivity and time resolution of FT-IR and detect much shorter lived intermediates. Efforts in this direction are underway in this laboratory and will be reported in due course.

ACKNOWLEDGMENT

This work was supported by ARPA.

Received for review January 30, 1995. Accepted September 13, 1995.[⊗]

AC9501046

[⊗] Abstract published in *Advance ACS Abstracts,* November 1, 1995.